APPLIED ORGANOMETALLIC CHEMISTRY
*Appl. Organometal. Chem.* 2003; **17**: 113–119
Published online in Wiley InterScience (www.interscience.wiley.com). DOI:10.1002/aoc.397



# Laser photolysis of trimethoxysilane: chemical vapour deposition of nanostructured silicone powders with Si—H and Si—$OCH_3$ bonds

**Radmila Tomovská[1], Zdeněk Bastl[2], Jaroslav Boháček[3] and Josef Pola[1]***

[1]Institute of Chemical Process Fundamentals, Academy of Sciences of the Czech Republic, 165 02 Prague, Czech Republic
[2]J. Heyrovský Institute of Physical Chemistry, Academy of Sciences of the Czech Republic, 182 23 Prague 8, Czech Republic
[3]Institute of Inorganic Chemistry, Academy of Sciences of the Czech Republic 250 68 Řež near Prague, Czech Republic

Received 5 August 2002; Accepted 4 November 2002

**Gas-phase photolysis of trimethoxysilane, achieved for the first time by focused ArF laser radiation at 193 nm, yields $C_{1,2}$ hydrocarbons, methanol and carbon monoxide along with ultrafine nanostructured silicone powder possessing —$SiO_3$ and $SiO_4$ configurations and Si—H and Si—$OCH_3$ bonds. The photolytic process, resulting in efficient removal of the methyl groups, is explained as a multitude of steps involving cleavages of all the available bonds. Copyright © 2003 John Wiley & Sons, Ltd.**

**KEYWORDS:** trimethoxysilane (TMOS); laser photolysis; nanostructured silicone powder

## INTRODUCTION

Silicon oxycarbides are continuously attracting attention owing to their significance in applied materials research (e.g. see Refs 1–4). Various Si–C–O and Si–C–H–O phases have been produced by pyrolysis of polysiloxanes (e.g. see Refs 5–7), polysiloxane gels (e.g. see Refs 8 and 9), pyrolytic IR laser–aerosol interaction[10] and plasma[11,12] or laser (e.g. see Refs 13–15) interaction with gaseous organosilanes.

We have recently reported on IR laser thermolysis[16–20] and UV laser-induced photolysis[21–23] of gaseous alkylhydridodisiloxanes resulting in chemical vapour deposition (CVD) of solid nanostructured silicones containing Si—H bonds.

It is known[24,25] that conventional UV photolysis of saturated Si—O-containing organosilanes at wavelengths below 200 nm is a very slow process controlled by cleavage of the weak Si—C bond. However, the photolysis of gaseous alkylhydridodisiloxanes achieved by intense laser radiation at 193 nm is a fast process that involves primary cleavage of the Si—C and Si—H bonds and secondary cleavage the Si—O bonds.[21–23] This photolysis is suitable for CVD of solid nanotextured silicones that are richer in H(Si) atoms than silicones obtained by IR laser thermolysis of disiloxanes. These silicones are thermally more stable than linear poly(dialkylsiloxanes).[21–23]

Intrigued by the possibility of altering the structure of the solid nanostructured silicone phases through using different precursors, we report in this paper on high-intensity ArF laser-induced gas-phase photolysis of trimethoxysilane (TMOS). We show that this process can be used for CVD of nanostructured silicone powders possessing —$SiO_3$ and $SiO_4$ configurations and containing Si—$OCH_3$ and Si—H bonds. These features make the solid a possible precursor to organically modified silicon oxides.

## EXPERIMENTAL

UV laser photolytic experiments were conducted in a stainless-steel or Pyrex reactor (140 ml in volume) consisting of two orthogonally positioned tubes (both 3.5 cm in diameter), one (13 cm long) fitted with two NaCl windows and the other (10 cm long) furnished with two quartz windows. These reactors were equipped with a port connecting them to a vacuum line, a PTFE valve and a port with rubber septum.

Some experiments were carried out in a Pyrex reactor made of a tube (2.2 cm in diameter, 10 cm long) furnished with a PTFE valve and tubing (1 cm in diameter, 8 cm long) perpendicularly attached to the tube and closed by a rubber septum. The tube had a pair of quartz windows (10 cm

*Correspondence to: J. Pola, Laser Chemistry Group, Institute of Chemical Process Fundamentals, Academy of Sciences of the Czech Republic, 165 02 Prague 6, Czech Republic.
E-mail: pola@icpf.cas.cz
Contract/grant sponsor: Ministry of Education, Youth and Sports of the Czech Republic; Contract/grant number: OC 523.60.

separation) and the tubing possessed a pair of NaCl windows (1.7 cm separation).

The reactors were filled with TMOS (68 Torr) and $N_2$ (total pressure 760 Torr) and in some runs with TMOS (68 Torr), *n*-propane (internal standard, 10 Torr) and $N_2$ at a total pressure of 760 Torr. An ArF (ELI 94 model) laser operated at 193 nm with a repetition frequency of 10 Hz and energy of 50–100 mJ effective on an area of 2 $cm^2$. The laser beam was focused with a quartz lens (focal length 25 cm) to obtain an incident fluence in the range of *ca* 0.1 –15.0 J $cm^{-2}$.

The progress of the photolysis was followed by periodically removing the reactor and placing it in the cell compartments of an FTIR (Nicolet Impact) spectrometer. The depletion of TMOS was monitored using diagnostic IR absorption bands at 1197 and 2206 $cm^{-1}$. The accumulation of gaseous products was followed by FTIR spectroscopy and by gas chromatography (Shimadzu GC 14A chromatograph coupled with a Chromatopac C-R5A computing integrator, Porapak P or SE-30 columns, programmed (20–150 °C) temperature, helium carrier gas). The volatile products were identified on a Shimadzu model QP 1000 quadrupole mass spectrometer (ionizing voltage 70 eV). Quantitative analyses of the volatile products relied on knowledge of the flame ionization detector response factors of the authentic samples. Carbon monoxide, methanol and ethyne were monitored using their respective IR bands at 2114 $cm^{-1}$, 1032 $cm^{-1}$ and 730 $cm^{-1}$.

In order to evaluate properties of the deposited solid product by FTIR spectroscopy, X-ray photoelectron spectroscopy (XPS) and electron microscopy, the deposited layers of the solid were produced on different substrates (KBr lumps, copper and aluminium sheets) accommodated in the reactor prior to irradiation.

Neat FTIR absorption spectra of the deposits were obtained after subtracting the spectra from that of TMOS. This procedure was required due to some residual adsorption of TMOS on the inner surface of the reactor, even after a prolonged evacuation of the reactor.

X-ray photoelectron spectra were recorded using an ESCA 310 (Gammadata Scienta) spectrometer and monochromatic Al Kα (1486.6 eV) radiation. The assignments of spectra to defined chemical states of elements are based on the comparison of measured and published[26–28] data. Calculation of the concentrations of elements was accomplished by correcting the photoelectron peak intensities for their cross-sections[29] and by accounting for the dependence of analyser transmission and electron inelastic mean free paths on their kinetic energies.[30] The samples were measured as received and after sputtering by argon ions ($E$ = 6 keV, $I$ = 20 μA, $t$ = 2 min). The aim of the ion sputtering was to remove the superficial layers, which could have been oxidized during sample transport from the reactor to the spectrometer.

Scanning electron microscopy (SEM) analyses were conducted on a Philips XL30 CP scanning electron microscope and transmission electron microscopy (TEM) photomicrographs were obtained using a Philips 201 transmission electron microscope.

TMOS was prepared by reaction of trichlorosilane with methanol in the presence of pyridine[31] and obtained by fractional distillation (b.p. 84 °C). Its purity was better than 98% as checked by gas chromatography.

## RESULTS AND DISCUSSION

ArF laser photolysis of TMOS in excess $N_2$ (TMOS absorptivity at 193 nm is $1 \times 10^{-3}$ $Torr^{-1}$ $cm^{-1}$) does not noticeably proceed with the unfocused radiation (incident fluence 0.2 J $cm^{-2}$) and is feasible only with incident fluences higher than 0.30 mJ $cm^{-2}$. The depletion of TMOS with laser pulses of the same energy is not affected by focusing the laser beam (Fig. 1). The photolysis results in the formation of volatile hydrocarbons, methanol and carbon monoxide, along with a white fog observed throughout all the inside of the reactor. The fog slowly deposits onto the reactor walls. At low irradiation fluence (0.30 mJ $cm^{-2}$) it produces an oily substance and at higher irradiation fluences (0.5–15 J $cm^{-2}$) it yields a white solid. The hydrocarbons observed are methane, ethane, ethene and ethyne, along with traces of butane. Their distribution (in relative mole percent) — $CH_4$ (60–70), $C_2H_4$ (3–15), $C_2H_6$ (25–30) and $C_2H_2$ (~1–2) — is similar for different incident fluences and somewhat dependent on the photolysis progress (Fig. 2). The yield of carbon monoxide, also being very similar with all the incident fluences, amounts to only *ca* 0.1–0.2 mol per mole of TMOS decomposed. The absence of any volatile silicon-containing compounds reveals that the silicon atom of TMOS is completely utilized for the formation of the materials deposited.

### Materials deposited

*Electron microscopy*

SEM images of the solid materials differ depending on the

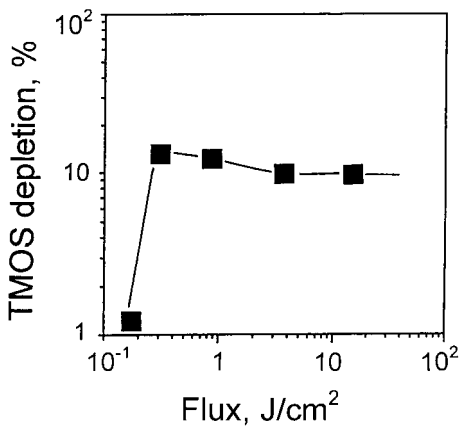


**Figure 1.** TMOS photolysis progress (after 600 pulses bearing energy of 70 mJ) versus incident fluence of laser radiation.

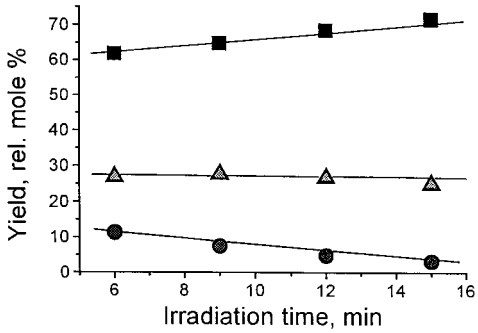


**Figure 2.** Dependence of relative yield of hydrocarbon on irradiation time ($F = 3.4$ J cm$^{-2}$): $CH_4$ (■), $C_2H_6$ (▲), $C_2H_4$ (●).

irradiation fluence used (Fig. 3). Those solids deposited at the highest fluence reveal a fluffy structure of bodies whose size is less than 1 μm; those deposited at a medium fluence show agglomerates of irregular shape, which are bonded together; and those solids deposited with a low fluence show a continuous morphology possessing some cracks. TEM analysis (Fig. 4) proved that all these materials can be described as agglomerates of several bodies with sizes of the order of tens of nanometres.

The formation of continuous structures at low fluence is in keeping with a view that transients produced at these conditions possess a higher polymerization ability than those generated under high fluence radiation.

### *XPS analysis*

The composition of the native solid deposits ($Si_{1.0}O_{1.7-2.0}C_{0.5-0.9}$) and of those sputtered by argon ions ($Si_{1.0}O_{1.5-1.6}C_{0.1-0.2}$) are given in Table 1. The binding energy of the Si (2p) electrons ($103 \pm 0.1$ eV) and the value of the modified Auger parameter ($1711.7 \pm 0.2$ eV) for as-received samples are close to the values for $SiO_2$ (103.4–103.6 and 1711.7–1712.2 eV),[26] $CSiO_3$ and $HSiO_3$ environments (both 102.8 eV).[27,28]

We thus assume that the silicon in the deposits is mostly contained in $XSiO_3$ (X = H, C) and $SiO_4$ configurations. Ion sputtering of the superficial layers of the deposits leads to an increase of the Auger parameter by only 0.4 eV, no change of the Si(2p) binding energy and a decrease of the oxygen and carbon concentrations by 15% and $73 \pm 4\%$ respectively. These findings indicate that the topmost layers were oxidized (and contaminated by adsorbed carbon-containing species) during their transfer from the reactor to the spectrometer. We can deduce that the powders contain $XSiO_3$

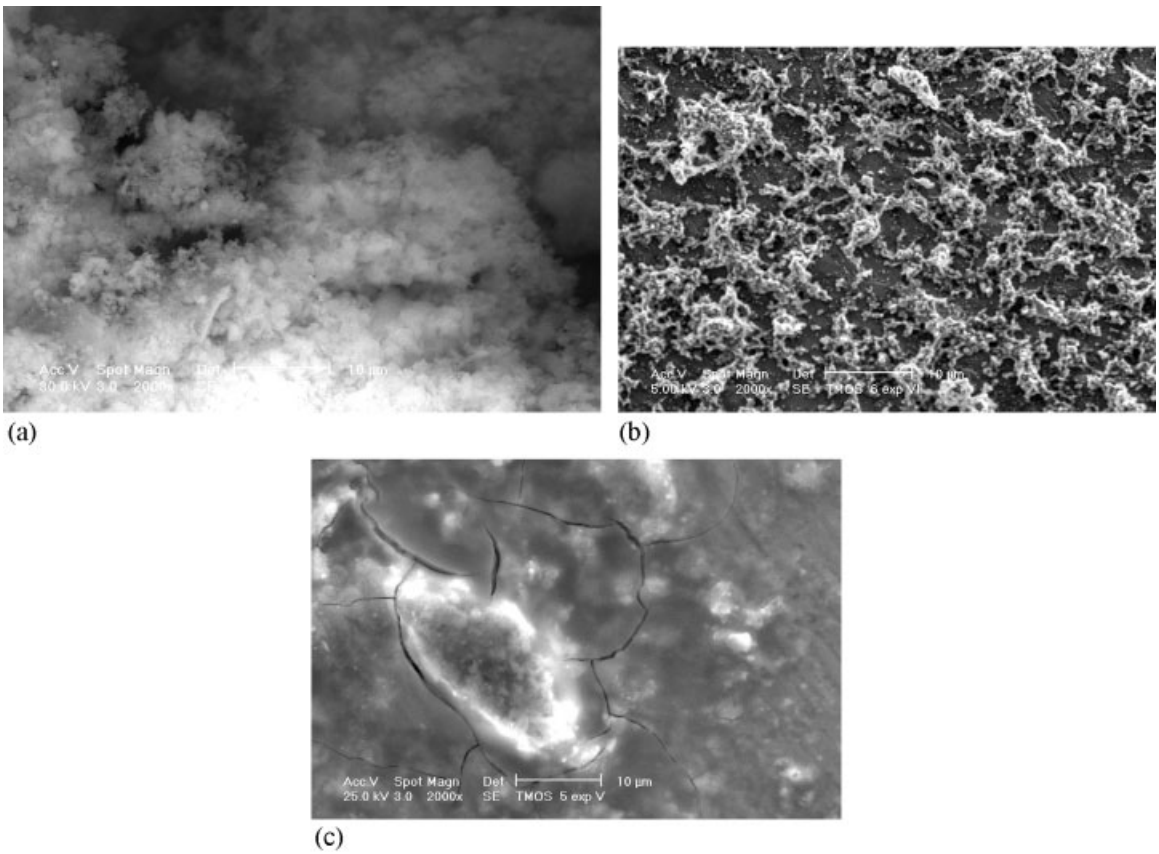


**Figure 3.** SEM of solid deposited at fluence of 14 J cm$^{-2}$ (a), 3.5 J cm$^{-2}$ (b) and 0.9 J cm$^{-2}$ (c). The bars are equal to 10 μm.

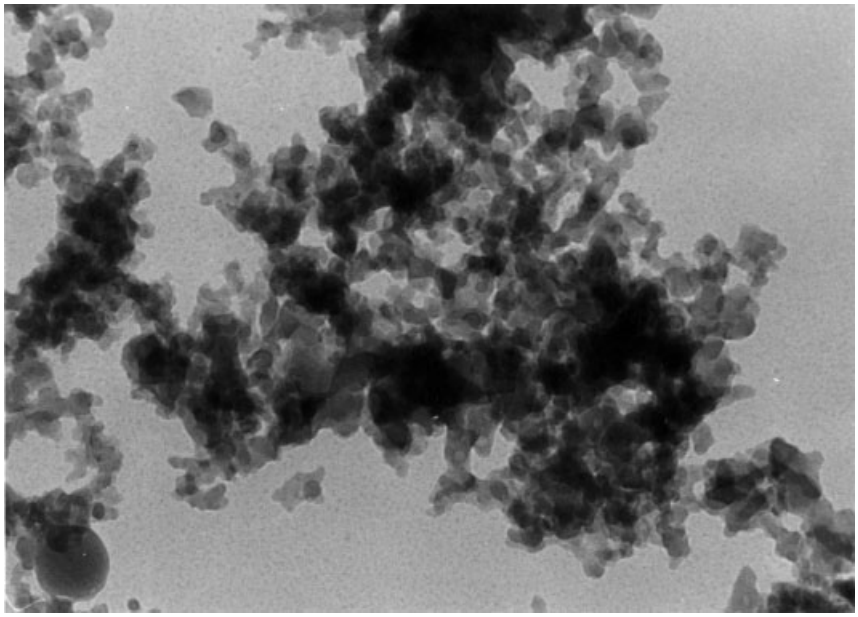

**Figure 4.** TEM image (×100 000) of solid deposited at fluence of 0.9 J cm$^{-2}$.

and $SiO_4$ configurations and that the —$SiO_3$ configuration undergoes oxidation in air.

## FTIR spectral analysis

The FTIR absorption spectra of the deposited films obtained with fluences 0.30–15.4 J cm$^{-2}$ show a similar pattern of bands assignable[32] to $\nu$(Si—C), $\delta$(Si—H), $\nu$(SiOC), $\nu$(SiOSi), $\rho(CH_3)$, $\nu$(Si—H) and $\nu$(C—H) vibrations (Fig. 5). They differ slightly in the relative absorbances of the individual bands, some of which are overlapping contributions of several vibrational modes (Table 2). The bands at 2953 and 2848 cm$^{-1}$ correspond to C—H stretches, the latter being characteristic of the stretching vibration of $CH_3$—O— groups. The $\nu$(Si—H) absorption band at 2227 cm$^{-1}$ is due[32–35] to the H—$SiO_3$ configuration, which is known[35] to have its bending mode at 875 cm$^{-1}$. The broad band centred at 1071 cm$^{-1}$ is composed of a band typical for the $\nu^{as}$(SiOSi) mode of branched siloxanes[32] (*ca* 1065 cm$^{-1}$) and that due to the $\nu$(Si—O—$CH_3$) mode, which typically appears[32] at 1100 cm$^{-1}$. The band at 884 cm$^{-1}$ is composed of contributions from the $\nu$(SiOC) and $\rho(CH_3)$ vibrational modes, and the band centred at 834 cm$^{-1}$ arises[32] from contributions from the $\delta$(H—$SiO_3$), $\nu$(Si—C) in siloxanes, $\nu(SiOCH_3)$ and $\rho(CH_3OSi)$ modes. Thus, the FTIR spectra unambiguously reveal the presence of $CH_3O$—Si, Si—O—Si, C—O—Si and H—$SiO_3$ moieties.

The absorptivity at the $\nu$(Si—H) and the $\nu$(C—H) vibrations is indicative of the distribution of hydrogen

**Table 1.** Stoichiometry of the deposits determined by XPS analysis

| Fluence (J cm$^{-2}$) | Sample | |
|---|---|---|
| | As received | Sputtered |
| 0.36[a] | $Si_{1.0}O_{2.0}C_{0.48}$ | $Si_{1.0}O_{1.60}C_{0.15}$ |
| 0.56[b] | $Si_{1.0}O_{1.77}C_{0.50}$ | $Si_{1.0}O_{1.55}C_{0.11}$ |
| 3.40[b] | $Si_{1.0}O_{1.75}C_{0.94}$ | $Si_{1.0}O_{1.59}C_{0.24}$ |
| 15.4[b] | $Si_{1.0}O_{1.7}C_{0.80}$ | $Si_{1.0}O_{1.45}C_{0.22}$ |

[a] Viscous oily material.
[b] Solid material.

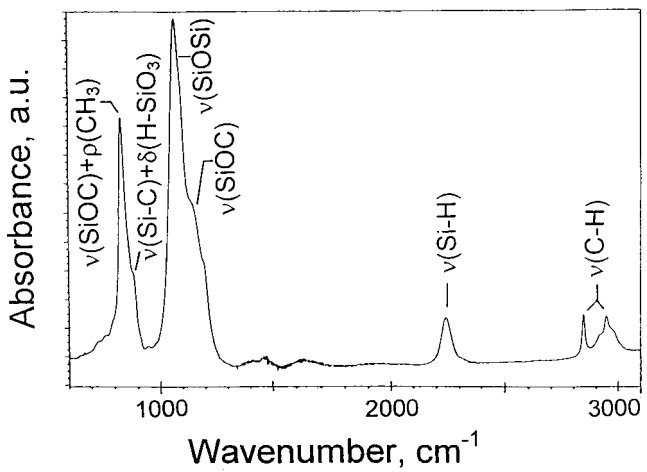


**Figure 5.** Typical FTIR spectrum of solid deposit.

**Table 2.** FTIR spectra of deposited materials[a] obtained at different irradiation fluence

| Absorption band [wavenumber ($cm^{-1}$)] | Absorbance[b] | | | |
|---|---|---|---|---|
| | $F$ = 15.4 J $cm^{-2}$ | $F$ = 3.40 J $cm^{-2}$ | $F$ = 0.56 J $cm^{-2}$ | $F$ = 0.36 J $cm^{-2}$ |
| $\nu$(Si—C) + $\delta$(H—$SiO_3$)[c] [834] | 0.41 | 0.25 | 0.18 | 0.72 |
| $\nu$(SiOC) + $\rho$($CH_3$) [884] | 0.29 | 0.21 | 0.12 | 0.19 |
| $\nu$(SiOSi) + $\nu$(SiOC) [1071] | 1.0 | 1.0 | 1.0 | 1.0 |
| $\nu$(Si—H) [2227] | 0.1 | 0.08 | 0.05 | 0.12 |
| $\nu^s$(C—H) [2848] | 0.05 | 0.04 | 0.01 | 0.07 |
| $\nu^{as}$(C—H) [2953] | 0.09 | 0.03 | 0.01 | 0.05 |

[a] Deposits at incident fluence of 15.4, 3.40 and 0.56 J $cm^{-2}$ are solids and that with fluence 0.36 J $cm^{-2}$ is an oily substance.
[b] Normalized to absorbance of the $\nu$(SiOSi) + $\nu$(SiOC) band.
[c] Overlap with $\nu$($SiOCH_3$), $\rho$($CH_3OSi$).[32]

atoms between the silicon and carbon centres;[36] the $A[\nu(C—H)]:A[\nu(Si—H)]$ ratio of the solids being (with one exception) $\geq 1$ shows that the concentration of the H(C) centres is about five times higher than that of the H(Si) centres.

Perusal of Table 2 shows that the relative absorbance of the $\nu$(SiOSi) + $\nu$(SiOC), $\nu^s$(C—H) and $\nu$(Si—H) bands declines with increasing incident fluence. This feature indicates that the content of the $CH_3O$(Si) and H(Si) constituents is higher at less intense radiation.

The FTIR spectra of the deposits exposed to air for several hours retain the same pattern, which implies that, apart from the oxidation of the topmost layers (see above), the deposits do not noticeably react at the Si—H and Si—$OCH_3$ bonds.

## Photolysis mechanism

The energy of the absorbed photons at 193 nm corresponds to *ca* 620 kJ $mol^{-1}$. This is much[37,38] in excess of the energy needed for cleavage of the C—O (*ca* 340 kJ $mol^{-1}$), Si—H (*ca* 380 kJ $mol^{-1}$), C—H (*ca* 410 kJ $mol^{-1}$), and Si—O (*ca* 530 kJ $mol^{-1}$) bonds and is also capable of inducing three-centre molecular elimination (*ca* 250–300 kJ $mol^{-1}$)[38] of methanol or Si—$OCH_3$/Si—H scrambling.[39] The possible occurrence of all these channels, which would make the total reaction scheme rather complex, is supported by available literature data on photolytic and thermal reactions of similar molecules.

The relative yields of the $C_1$–$C_2$ hydrocarbons ($CH_4 \gg C_2H_6 > C_2H_4$) in the photolysis reveal the importance of the Si—O homolysis, the formation of $CH_3$ radicals and the abstraction by these radicals of H(Si), which is preferred[40–42] to that of H(C).

The observed ethane, ethene and ethyne result from known reactions ($2CH_3^{\bullet} \rightarrow C_2H_6$, $CH_3^{\bullet} \rightarrow :CH_2 + H$, $2{:}CH_2 \rightarrow C_2H_4$, $C_2H_4 \rightarrow C_2H_2 + H_2$). The relative yield of ethane is virtually independent of the photolysis process, but that of ethene decreases and that of methane increases (Fig. 2). This is in line with a continuously increasing importance of H-abstraction by the $CH_3$ radicals and is related to a more feasible formation of $CH_3$ radicals from photolytic products than from TMOS. The insignificant occurrence of ethyne, a typical 'hot' photolytic product, is due to effective vibrational deactivation of hot ethene molecules by excess nitrogen.

Methanol can originate either from the homolysis of the strongest Si—O bonds and subsequent H-abstraction by the $CH_3O$ radical, or via an as yet unobserved (and less energy demanding) 1,1-$CH_3OH$ elimination. The latter path may consist[43] of simultaneous formation of $CH_3O$ and H radicals that recombine within the molecular sphere. Similar 'molecular extrusions' were reported[44–46] for laser-induced photolysis of organometallic compounds.

The observation of CO and the absence of gaseous $H_2CO$ or solid paraformaldehyde among the products is compatible[47] with photolysis of methanol into formaldehyde and molecular hydrogen and further to CO and molecular hydrogen. Independent photolysis of CO at 293 nm revealed that this compound is stable under the conditions used.

The plausible reaction steps, i.e. homolysis of the O—C, Si—H and C—H bonds of TMOS (Eqns (1)–(3)), $\beta$-cleavages of the produced O- and Si-centred radicals (Eqns (5), (6) and (8)), three-centre molecular elimination of methanol (Eqn. (4)), as well as abstraction of the H(Si) atom from TMOS (Eqn. (7)), are depicted in Scheme 1. These reactions and elimination of formaldehyde from the C-centred radical[48] (Eqn. (10)) lead to smaller radicals, dimethoxysilylene and dimethoxysilanone (Eqns (7) and (8)), all of which can take part in a multitude of association reactions producing macromolecules (Eqns (9) and (11)). A loss of oxygen and carbon from these products can occur via reactions (12)–(15) (Scheme 1). The decay of methanol is described via the sequence of steps (16) and (17).[48] All these reactions can be accompanied with cleavage of the strong Si—O bond, which is normally a difficult primary photochemical event,[24,25] but is one that can be viable upon multi-photon absorption with high-intensity laser radiation, even though the fission of the weaker linkages is to be preferred.

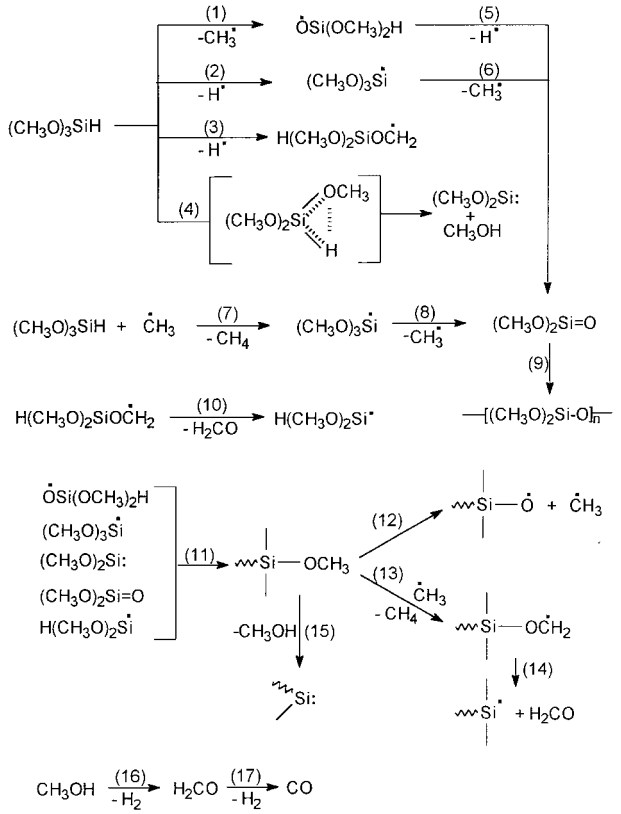

**Scheme 1.**

## CONCLUSION

Gas-phase photolysis of TMOS achieved with highly focused radiation from an ArF laser yields $C_1$–$C_2$ hydrocarbons, methanol and carbon monoxide together with a solid nanostructured Si–C–H–O material containing —$SiO_3$ and $SiO_4$ configurations and Si—H and Si—$OCH_3$ bonds. The multitude of steps leading to the solid material takes place within a period of milliseconds in a small region of the laser beam. Under these conditions, i.e. room temperature of the total gaseous volume being maintained, the procedure makes possible the deposition of nanostructured phases on cold substrates. The production of silicon oxide layers with interesting properties (high resistance to oxygen and water, gas selectivity) at room temperatures (rather than at pyrolytic temperatures) is attracting interest,[49] and the reported photolytic degradation of TMOS can become important in this respect. Moreover, the solid silicone powder containing Si—H and Si—$OCH_3$ bonds can be further chemically modified by hydrosilylation and esterification reactions. These features make the deposited silicone an interesting precursor to silicon oxides modified[50,51] with large organic groups.

## Acknowledgements

This work was supported by the Ministry of Education, Youth and Sports of the Czech Republic (Program COST, no. OC 523.60). A NATO postdoctoral fellowship to R.T. is gratefully acknowledged.

## REFERENCES

1. Hurwitz FI, Heimann P, Farmer SC and Hembree DM. *J. Mater. Sci.* 1993; **28**: 6622 and references cited therein.
2. Breval E, Hammond H and Pantano CG. *J. Am. Ceram. Soc.* 1994; **77**: 3012.
3. Soraru GD, Liu Q, Interrante LV and Apple T. *Chem. Mater.* 1998; **10**: 4047.
4. Bois L, Maquet J, Babonneau F, Mutin H and Bahloul D. *Chem. Mater.* 1994; **6**: 796.
5. Wilson AM, Zank G, Eguchi K, Xing W, Yates B and Dahn JR. *Chem. Mater.* 1997; **9**: 1601.
6. Mantz RA, Jones PF, Chaffee KP, Lichtenhan JD, Gilman JW, Ismail IMK and Burmeister MJ. *Chem. Mater.* 1996; **8**: 1250.
7. Kurjata J, Scibiorek M, Fortuniak W and Chojnowski J. *Organometallics* 1999; **18**: 1259.
8. Babonneau F. *Polyhedron* 1994; **13**: 1123.
9. Dire S, Campostrini R and Ceccato R. *Chem. Mater.* 1998; **10**: 268.
10. Kortobi YE, Esoinose de la Caillerie J-B, Legrand AP, Armand X, Herlin N and Cauchetier M. *Chem. Mater.* 1997; **9**: 632.
11. Fujii T, Yokoi T, Hiramatsu M, Nawata M, Hori M, Goto T and Hattori S. *J. Vac. Sci. Technol. B* 1997; **15**: 746.
12. Bartella J and Herwig U. *Fresenius Z. Anal. Chem.* 1993; **346**: 351.
13. Alexandrescu R, Morjan J, Grigoriu C, Bastl Z, Tláskal J, Mayer R and Pola J. *Appl. Phys. A* 1988; **46**: 768.
14. Pola J, Čukanová D, Minárik M, Lyčka A and Tláskal J. *J. Organomet. Chem.* 1992; **426**: 23.
15. Pola J and Morita H. *Tetrahedron Lett.* 1997; **38**: 7809.
16. Pola J, Urbanová M, Dřínek V, Šubrt J and Beckers H. *Appl. Organomet. Chem.* 1999; **13**: 655.
17. Pola J, Urbanová M, Bastl Z, Šubrt J and Papagiannakopoulos P. *J. Mater. Chem.* 2000; **10**: 1415.
18. Pola J, Urbanová M, Bastl Z and Beckers H. *Appl. Organomet. Chem.* 2000; **14**: 453.
19. Kupčík J, Bastl Z, Šubrt J, Pola J, Papadimitriou VC, Prosmitis AV and Papagiannakopoulos P. *J. Anal. Appl. Pyrol.* 2001; **57**: 109.
20. Urbanová M, Bastl Z, Šubrt J and Pola J. *J. Mater. Chem.* 2001; **11**: 1557.
21. Pola J, Urbanová M, Bastl Z, Šubrt J and Beckers H. *J. Mater. Chem.* 1999; **9**: 2429.
22. Pola J, Ouchi A, Šubrt J, Bastl Z, Sakuragi M, Galíková A and Galík A. *Adv. Mater. Chem. Vap. Depos.* 2001; **7**: 19.
23. Pola J, Galíková A, Galík A, Blechta V, Bastl Z, Šubrt J and Ouchi A. *Chem. Mater.* 2002; **14**: 144.
24. Dalton JC. In *Organic Photochemistry*, vol. **7**, Padwa A (ed.). Marcel Dekker: New York, 1985; chapter 3.
25. Schumann H-P, Ritter A and von Sontag C. *J. Organomet. Chem.* 1978; **148**: 213.
26. *X-Ray Photoelectron Spectroscopy Database*, Ver. 2.0. NIST: Gaithersburg, 1997.
27. Alexander MR, Short RD, Jones FR, Stollenwerk M, Zabold J and Michaeli W. *J. Mater. Sci.* 1996; **31**: 1879.
28. Alexander MR, Short RD, Jones FR, Stollenwerk M, Michaeli W, Blomfield CJ. Determination of the structure of HMDSDO/O2 plasma deposits using high resolution XPS. In *43rd AVS National Symposium*, Philadelphia, PA, 1996.
29. Scofield JH. *J. Electron Spectrosc.* 1976; **8**: 129.
30. Seah MP and Dench WA. *Surf. Interface Anal.* 1979; **1**: 1.
31. Klejnot OJ. *Inorg. Chem.* 1963; **2**: 825.
32. Miller RGJ, Willis HA (eds). *Infrared Structural Correlation Tables and Data Cards*. Heyden: Spectrum House, London, 1969; Table 9.

33. Tsu DV, Lucovsky G and Davidson BN. *Phys. Rev. B*. 1989; **40**: 1795.
34. Lucovsky G, Nemanich RJ and Knights JC. *Phys. Rev. B*. 1979; **19**: 2064.
35. He L, Inokuma T, Kurata Y and Hasegawa S. *J. Non-Cryst. Solids* 1995; **185**: 249.
36. Low HC and John P. *J. Organomet. Chem.* 1980; **201**: 363 and references cited therein.
37. Walsh R. In *The Chemistry of Organic Silicon Compounds*, Patai S, Rappoport Z (eds). Wiley: Chichester, UK, 1989; chapter 5.
38. Benson S. *Thermochemical Kinetics*. Wiley: New York, 1976.
39. Moedritzer K. *Organomet. Chem. Rev.* 1966; **1**: 179.
40. Kerr JA, Slater DH and Young JC. *J. Chem. Soc. (A)* 1967; 134.
41. Kerr JA, Slater DH and Young JC. *J. Chem. Soc. (A)* 1966; 104.
42. Morris ER and Thynne JC. *J. Phys. Chem.* 1969; **73**: 3294.
43. Pola J, Parsons J and Taylor R. *J. Chem. Soc. Faraday Trans.* 1992; **88**: 1637.
44. Beuermann T and Stuke M. *Appl. Phys. B* 1989; **49**: 145.
45. Pola J and Taylor R. *J. Organomet. Chem.* 1992; **437**: 271.
46. Pola J and Taylor R. *J. Organomet. Chem.* 1993; **446**: 131.
47. Calvert JG, Pitts JN. *Photochemistry*. Wiley: New York, 1966.
48. Chu JCS, Soller R, Lin MC and Melius CF. *J. Phys. Chem.* 1995; **99**: 663.
49. Ouyang M, Yuan C, Muisenger RJ, Boulares A and Koberstein JT. *Chem. Mater.* 2000; **12**: 1591.
50. Hay J, Porter D and Raval H. *Chem. Commun.* 1999; 81.
51. Tao T and Maciel GE. *J. Am. Chem. Soc.* 2000; **122**: 3118.

 